
BUDAPEST, JUNE, 2026

Status and Upgrades of the MuGrid-v2 Detector Muographers 26

Tao Yu, Yunsong Ning, Yi Yuan , Shihan Zhao,
Songran Qi , Mingchen Sun , Zhirui Liu , Aiyu Bai,
Yu Chen, Jian Tang

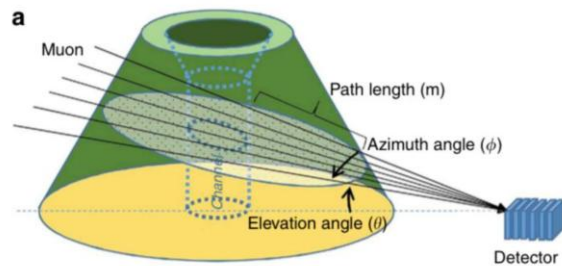
SUN YAT-SEN UNIVERSITY



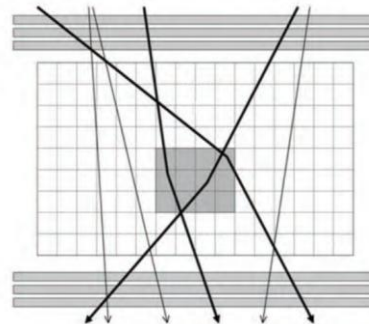
中山大學
SUN YAT-SEN UNIVERSITY

Cosmic-ray Muon & transmission muography

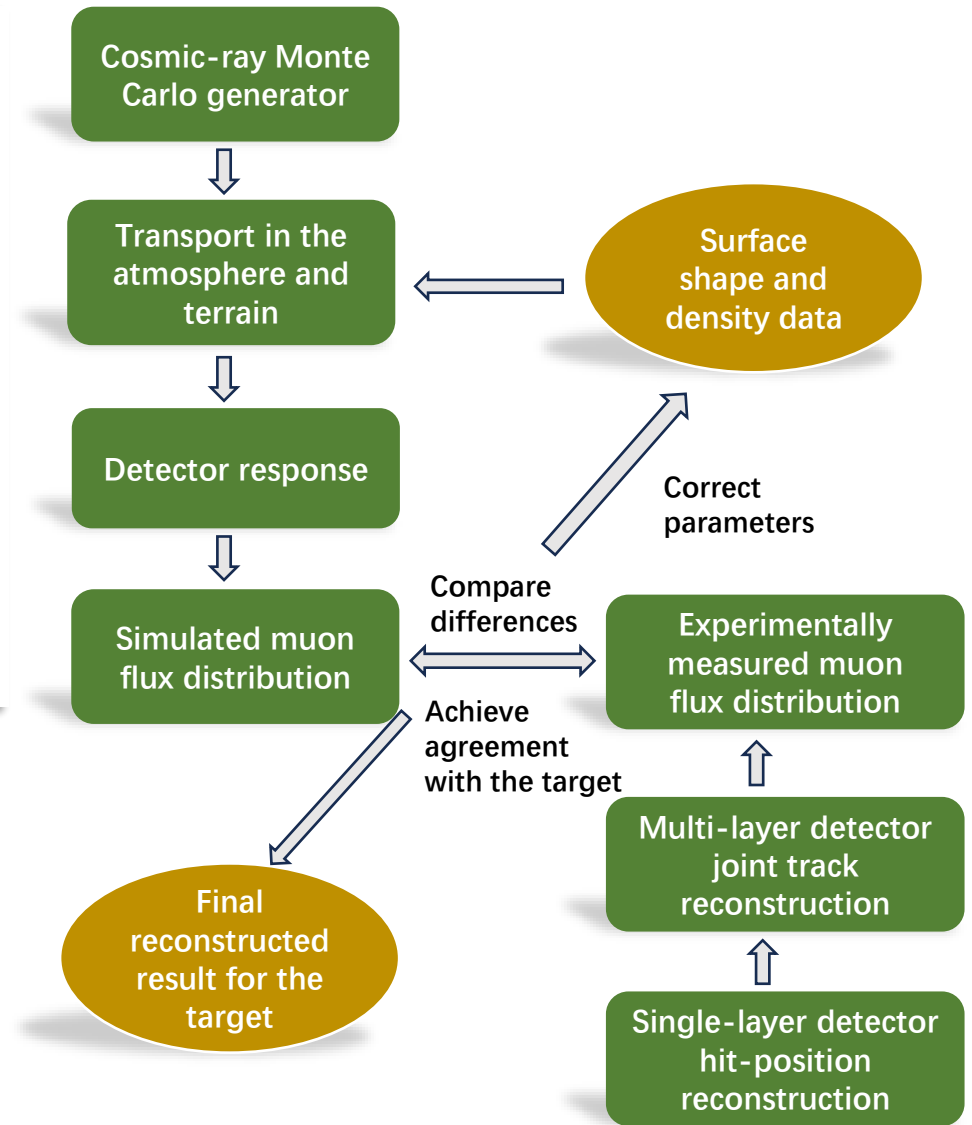
- Cosmic-ray muons are secondary particles produced by interactions between primary cosmic rays and the air.
- Internal structure imaging enabled by muon energy loss during material penetration.
- Muography can generally be divided into:
 - Scattering imaging: Sensitive to high-Z anomalies
 - Transmission imaging: Suitable for large-volume object inspection



transmissing muography



Scattering muography

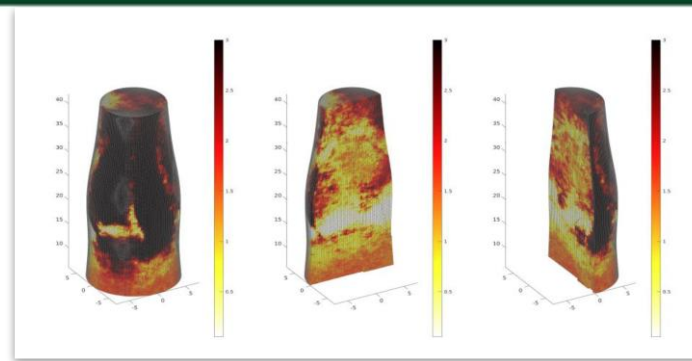


Multidisciplinary Applications of muography

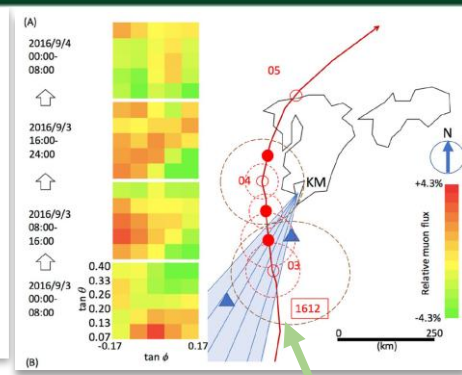


➤ Archaeology

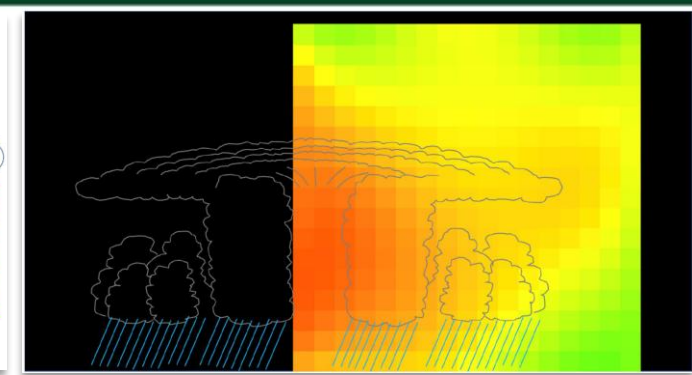
Kunihiro Morishima, et al
Nature 552, 386–390 (2017)



➤ Blast furnace inspection
Cohu et.al
JINST 18 (2023) 07, P07004



➤ Typhoon warning



H.K.M Tanaka, et al
Scientific Reports 12, 16710 (2022)

Muography has shown rapidly growing potential across multiple disciplines!

- Gas detectors
- High spatial resolution & Large-area coverage
 - typically need continuous gas supply

➤ Sea-level monitoring



H.K.M Tanaka, et al
Scientific Reports 11, 19485 (2021-09)

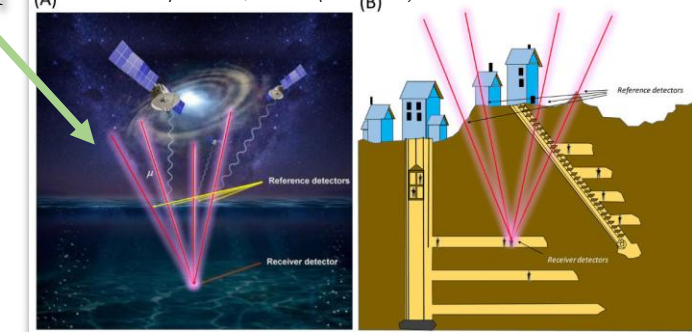
➤ Volcano monitoring



M. Derrico, F. Ambrosino et al
arxiv:2202.12000

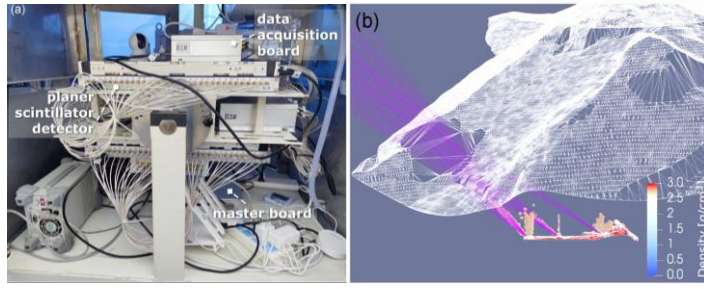
- Nuclear emulsion detectors
- Ultra-high spatial resolution
 - melting under high-temperature

➤ Underwater navigation



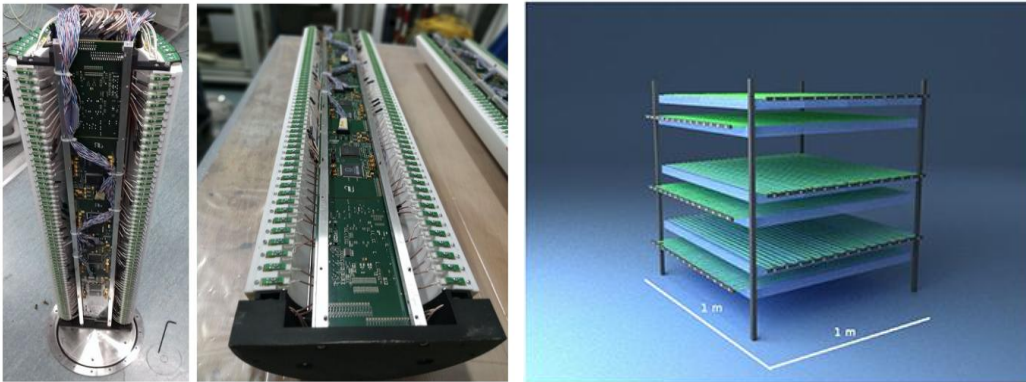
H.K.M Tanaka, et al
Scientific Reports 13, 15272 (2023)

- Scintillator detectors
- mm-level spatial resolution
- Geological exploration • Robust and environmentally adaptable

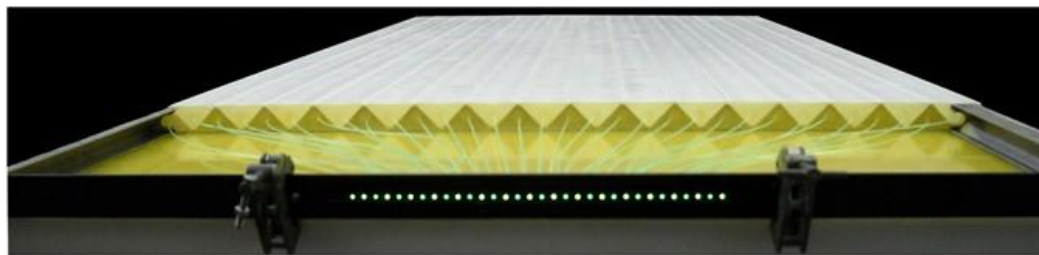


Guorui Liu et al
Geophysical Journal International, Vol. 237, 588-603

Conventional plastic-scintillator detector configurations



semicircular *G. Saracino et al Sci Rep 7, 1181 (2017)* **Rectangular** *M. Niculescu-Oglinzanu et al J. Appl. Phys. 136, 174501 (2024)*

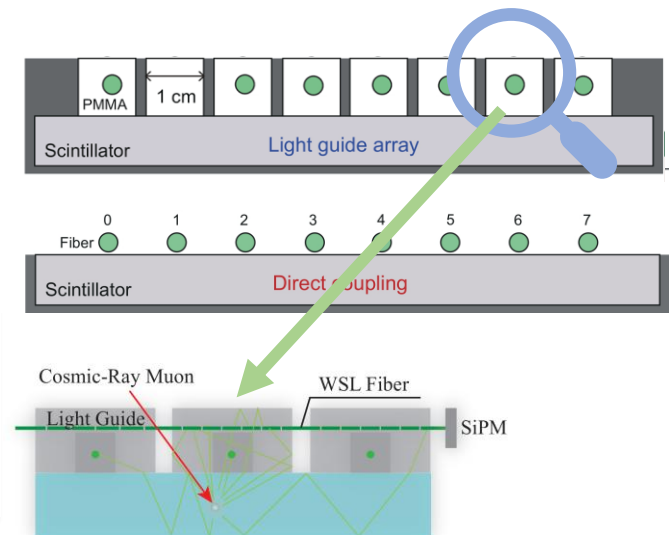
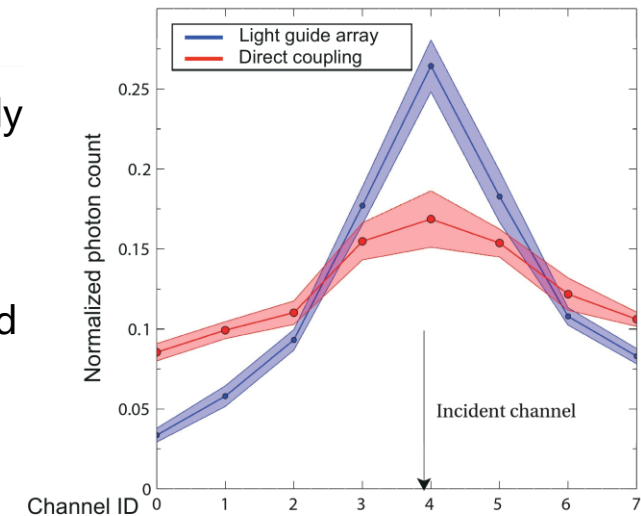


Triangular

A. Anastasio et al NIMA 732 (2013) 423-426

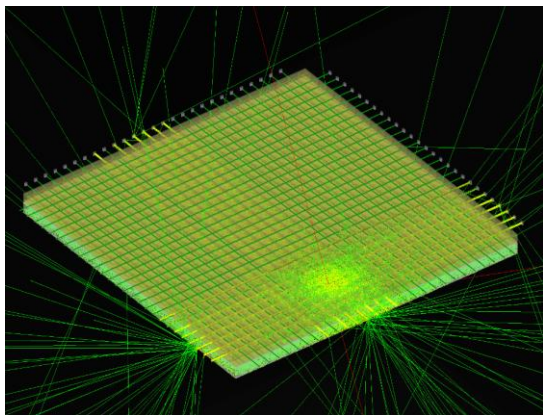
These are all excellent detector solutions, but scalability and production cost remain important challenges.

- Use Light-guide arrays to optically segment the scintillator without physical cutting.
- Scintillation photons are collected by WLS fibers and read out by edge-mounted SiPMs
- Two-dimensional light-intensity distributions can be obtained from the X and Y fiber arrays.
- Muon hit positions can be reconstructed by centroid methods or Gaussian fitting.
- Easily achieve X and Y readout on a single scintillator block.



Hang Yang, Yao Yu, et al NIMA 1042 (2022) 167402

MuGrid-v2 Simulation comparison

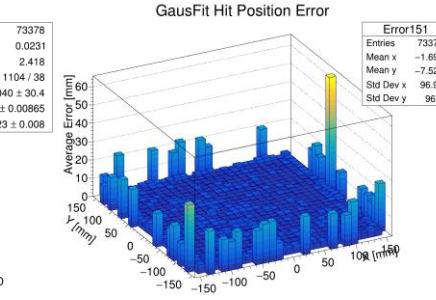
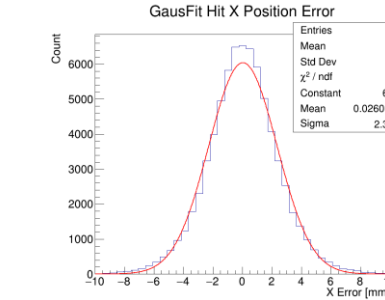
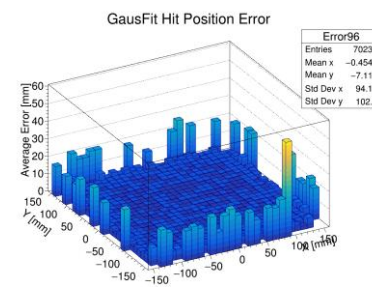
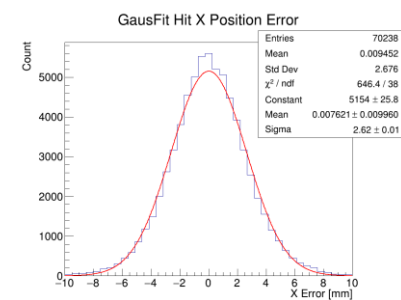
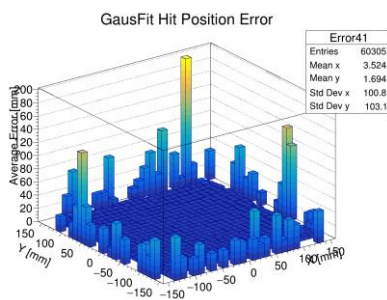
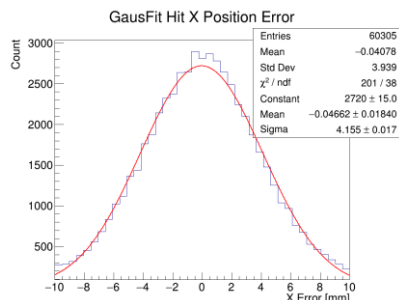
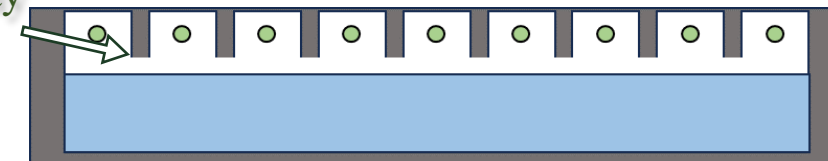
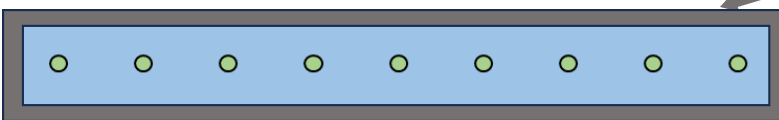


Geant4 visualization

- Geant4 simulations were conducted on the three coupling modes of WSL fibers: **surface coupling, internal coupling, light guide array.**
- The scintillator size is 30cm*30cm, with 27 channels per direction (11mm gap) .

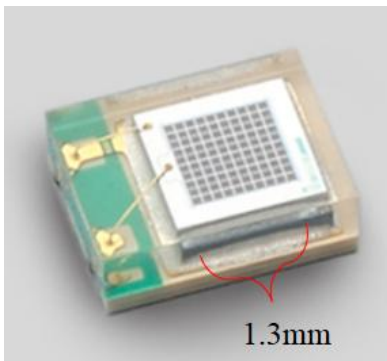
High cross talk

Low efficiency



Coupling method	Internal	Surface	Light guide
Reconstruction methods			
Resolution of centroid/mm	15.46 ± 0.82	3.576 ± 0.012	2.706 ± 0.009
Resolution of fitting/mm	4.155 ± 0.017	2.62 ± 0.015	2.323 ± 0.008

➤ SiPM



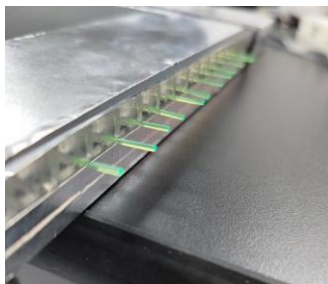
➤ S13360 series

- Size: 1.3mm × 1.3mm
- Gain: 1.7×10^6
- V_{BR} : 53 ± 5 V

➤ WLS fiber

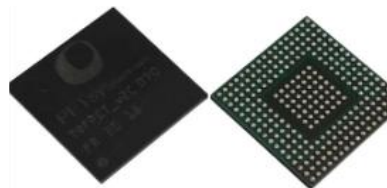
➤ Kuraray Y-11

- Emission Peak: 476 nm
- Attention Length: 3.5 m
- good spectral matching



Use cosmic-ray muons to test the uniformity of channel responses and repair abnormal channels.

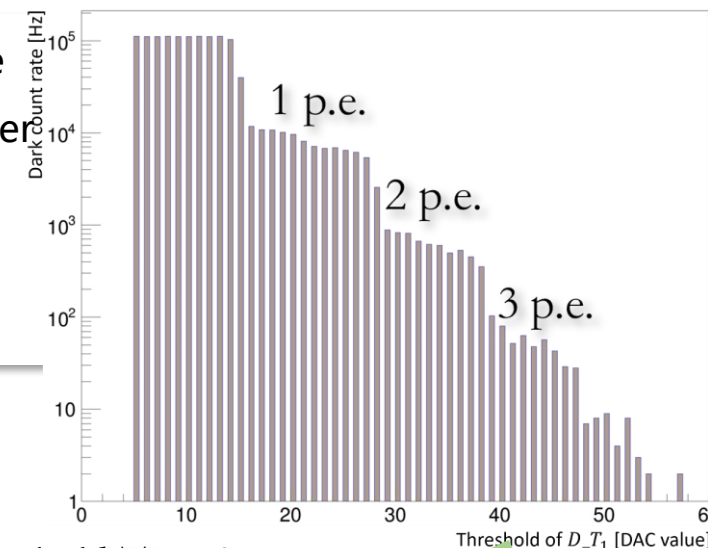
➤ ASIC



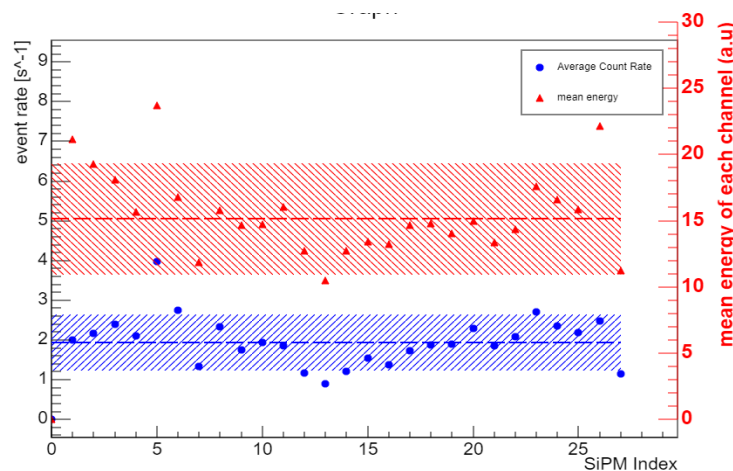
Count dark count rate to calibrate the number of photoelectrons corresponding to the threshold

TOFPET2 ASIC features

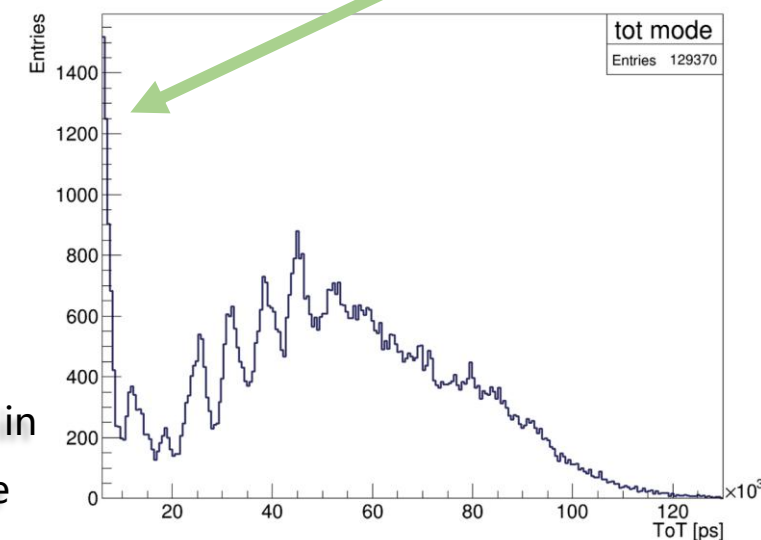
- 64 independent channels
- TDC time binning: 30 ps.
- Max channel hit rate: 600 kHz
- Dynamic range: 1500 pC.



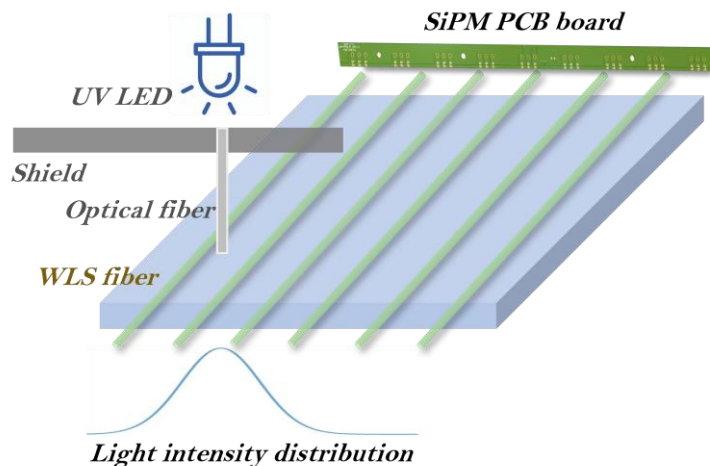
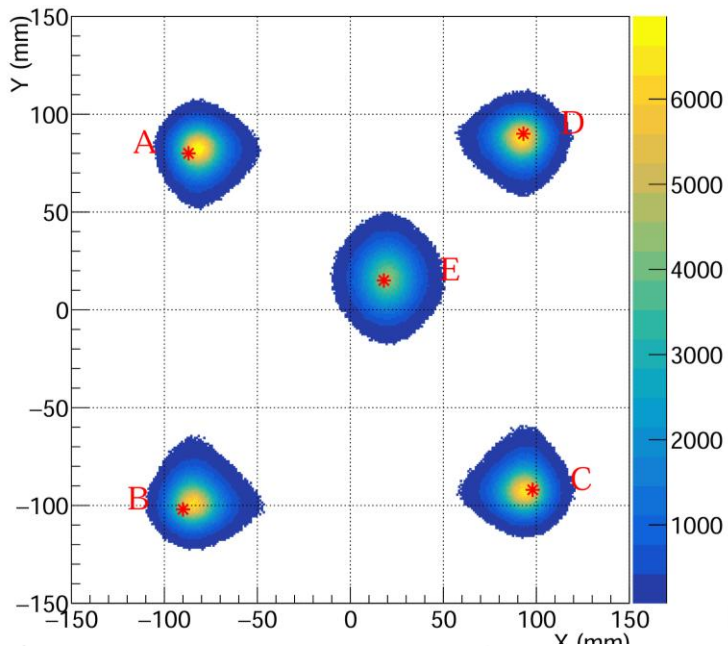
Threshold $T_1=43$



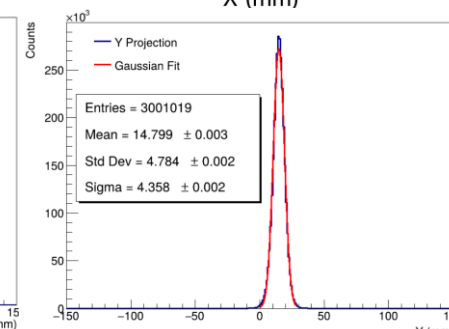
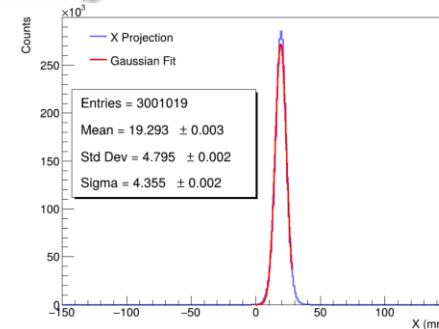
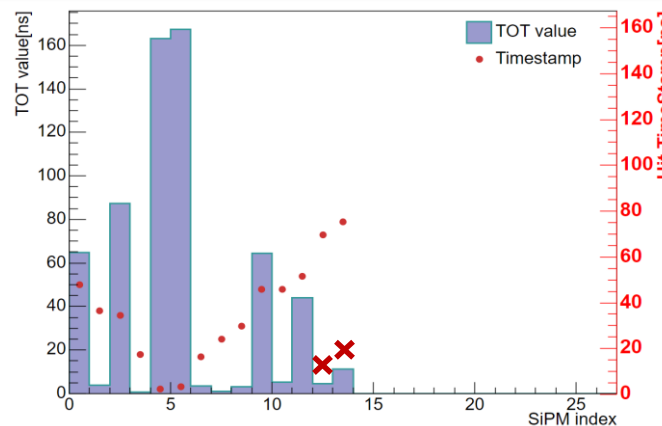
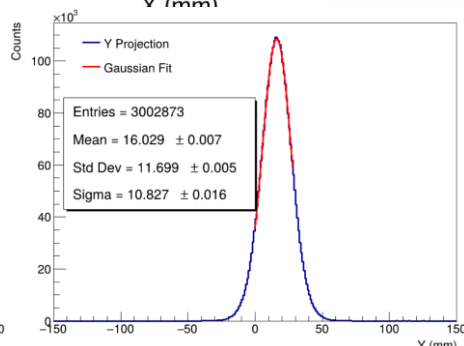
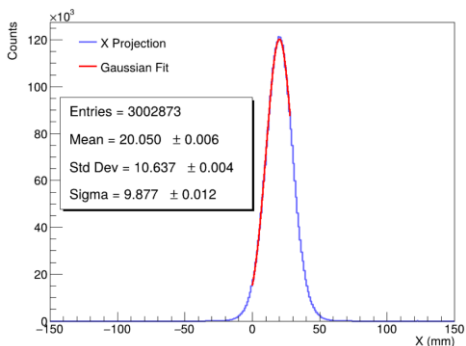
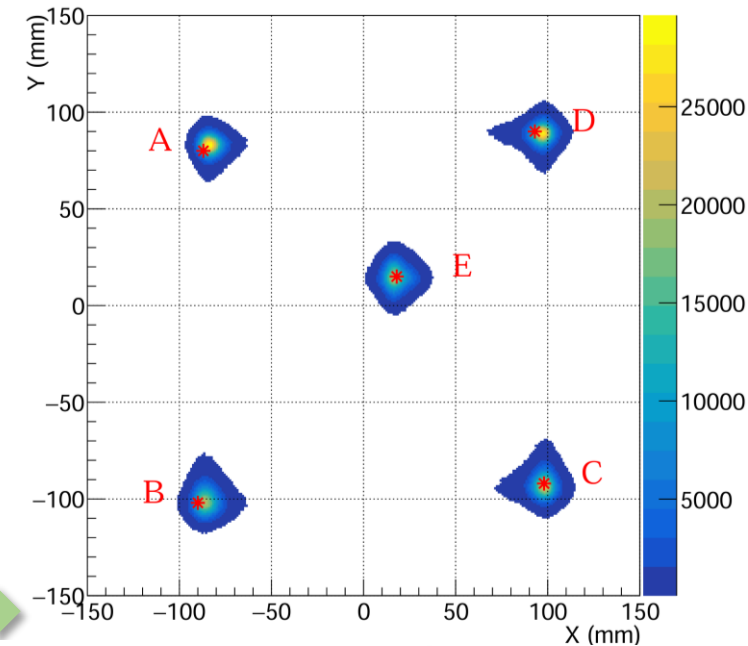
Multi p.e. spectrum in TOT mode



MuGrid-v2 Reconstruction algorithm



Calibrate the spatial resolution with LED in 5 points on the scintillator

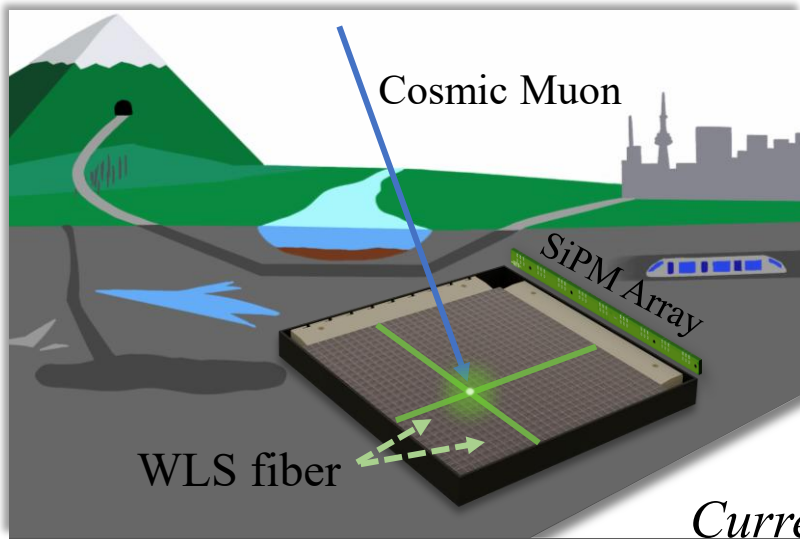


$$\hat{X} = \frac{\sum E_i X_i}{\sum E_i}$$

For trigger channels farther from the hit point, the timestamp will be further late

$$\hat{X} = \frac{\sum \frac{E_i X_i}{\sqrt{1+(t_i/\sigma_t)^2}}}{\sum \frac{E_i}{\sqrt{1+(t_i/\sigma_t)^2}}}$$

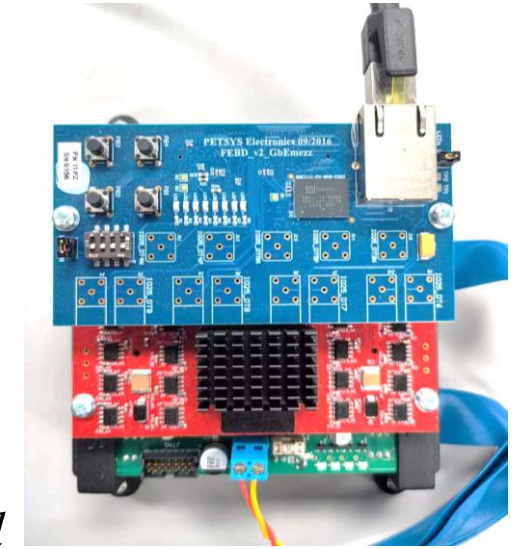
MuGrid-v2 workflow



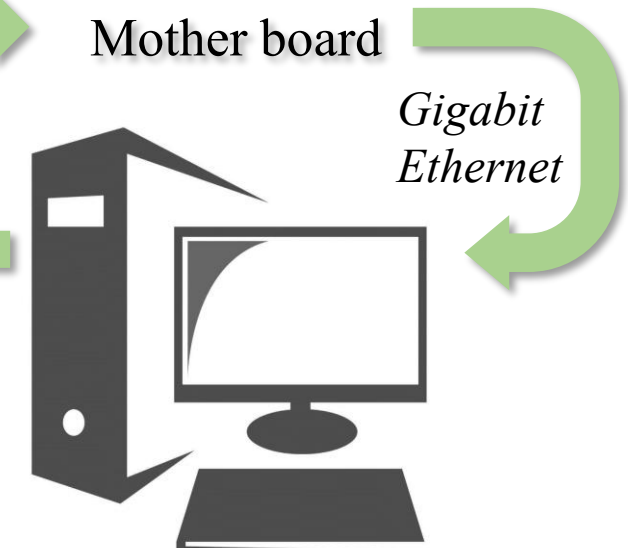
MuGrid detector



FEB module &
TOFPET2 ASIC



Mother board



Upper computer

Current signal



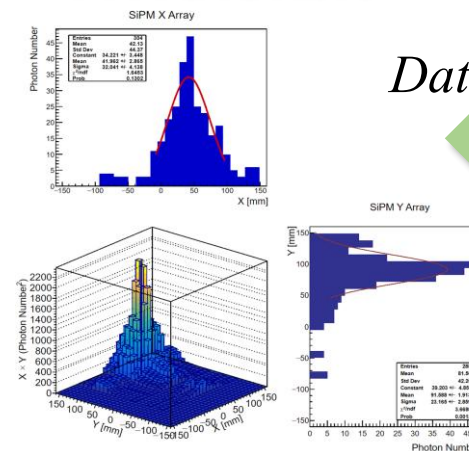
Digital signal



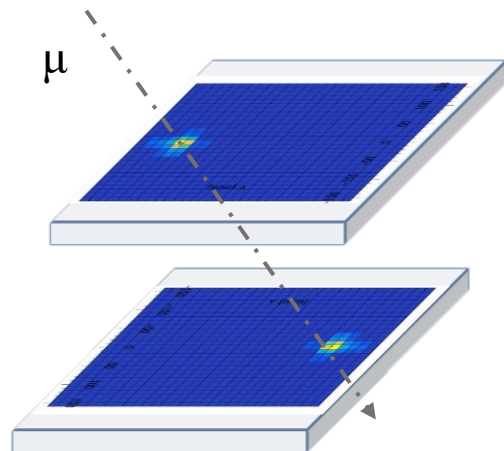
Data acquisition



Analysis



Hit position reconstruction



Track reconstruction

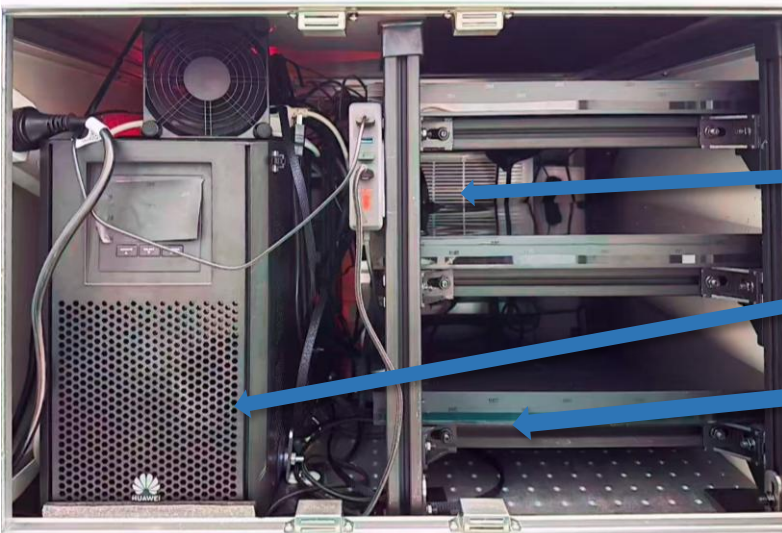
MuGrid-v2 open-sky measurement



Three-layer Detector integrated into a protective box, equipped with a UPS for power security, an air conditioner for temperature control and a WIFI module for remote control.

- Dimensions: 1.4m×0.8m×0.55m
- Total Weight: ~50kg
- Power Consumption: ~120W(mainly driven by the AC unit)

Monitoring camera

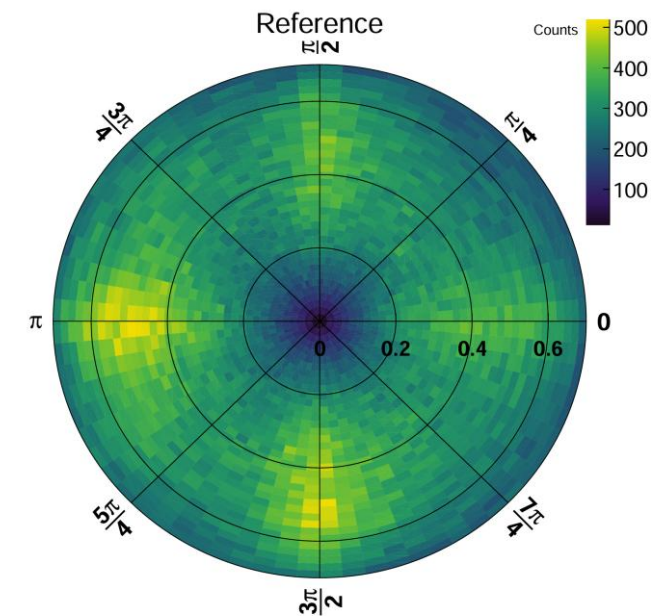


Air conditioning

UPS Power

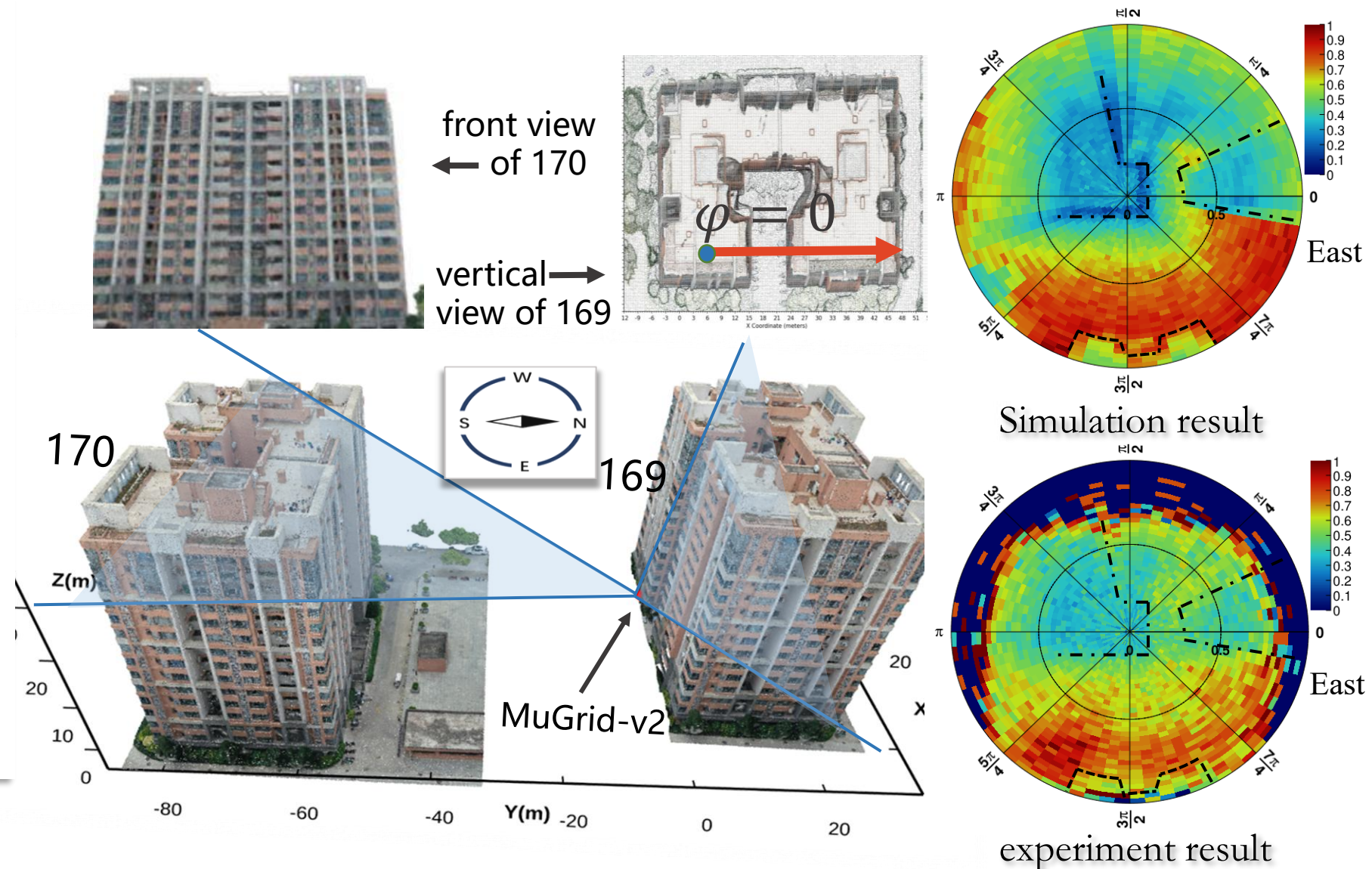
MuGridv2 detector

90hours of open-sky muon flux were collected. Because the detector is square, there is some flux enhancement in the four directions.



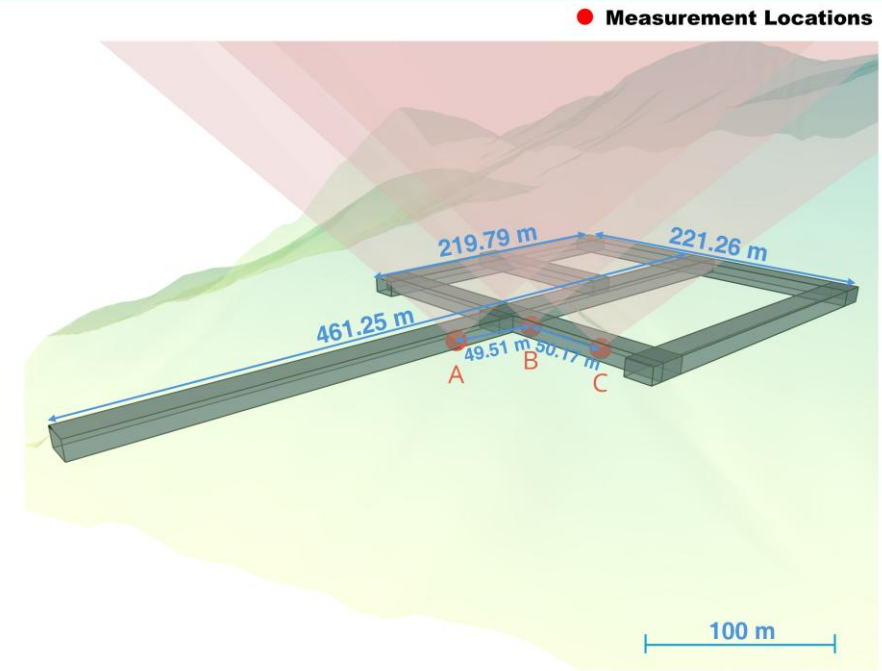
Case study: Dormitory building shadow

- Drone scanning was used to obtain 3D models of the two dormitories
- The detector is placed in a room on the south side of the first floor of Building 169.
- Significant muon flux reduction observed on the north side due to shielding by Building 169
- Flux suppression at low elevation angles on the south side caused by Building 170



Case study: Tianqin tunnel terrain inversion

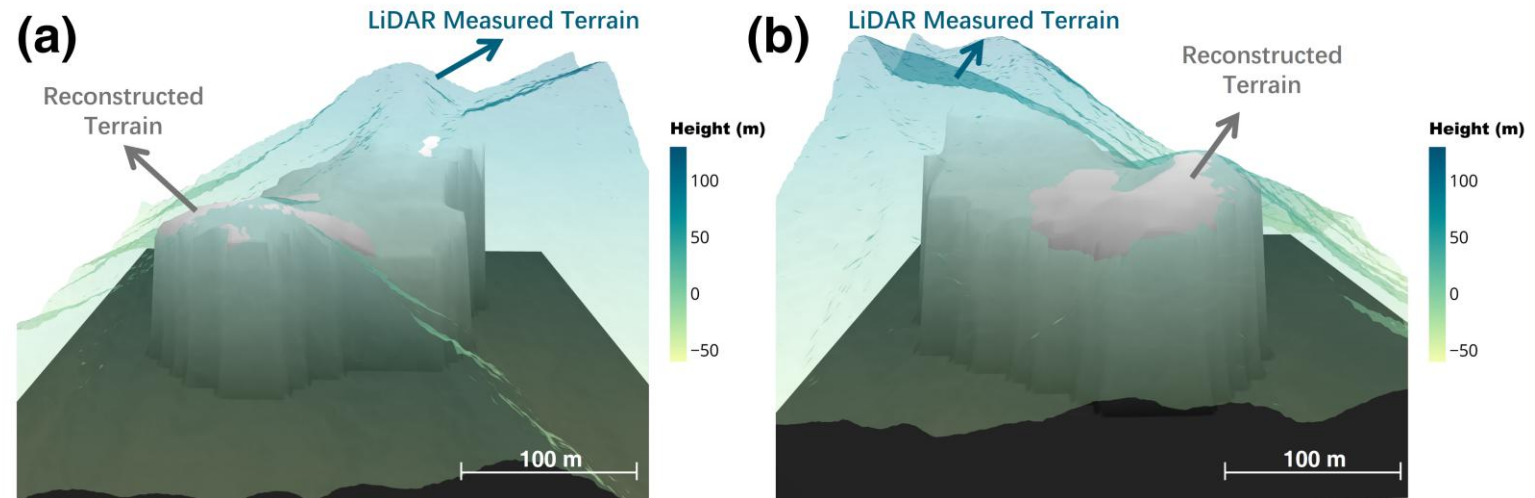
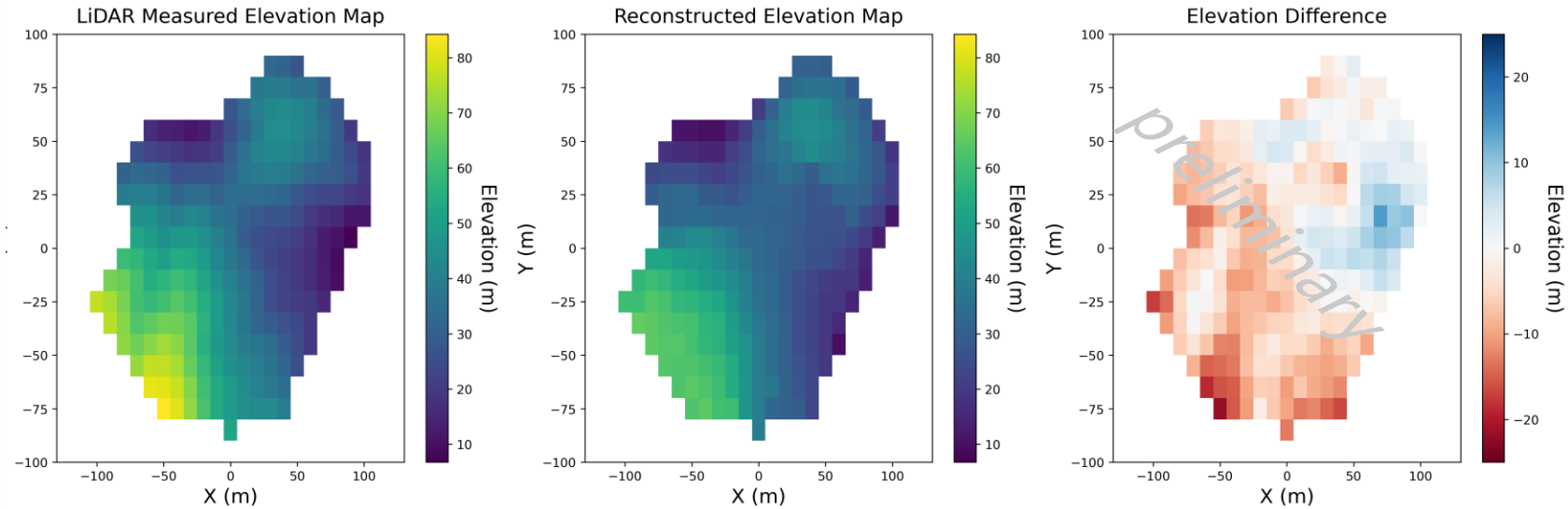
- We try to perform 3D reconstruction of the mountain's orientation within the detector's field of view.
- 3D topographic model of Tianqin tunnel constructed using LiDAR measured terrain data .
- Detector deployed in three laboratories (A, B, and C) for 7, 14, and 15 days, collecting 10,727, 24,405, and 17,909 valid muon events, respectively



Debugging and measuring location coordinates inside the tunnel

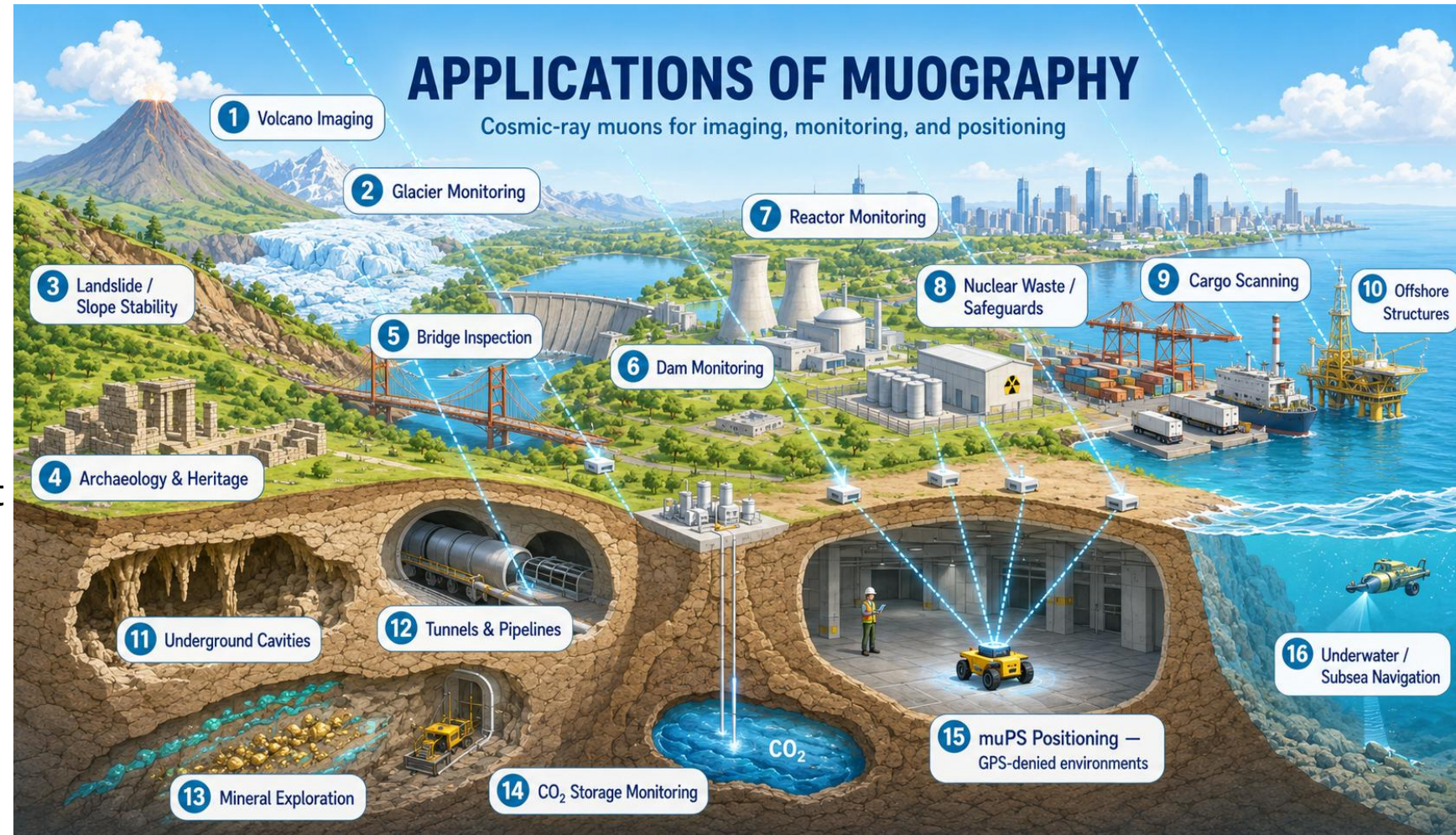
Case study: Tianqin tunnel terrain inversion

- Colored shell represents the real terrain data. Black-and-white columns represent the reconstructed results
- the reconstructed terrain successfully reproduced the main topographical features overall.
- Mean absolute error: approximately 7m.
- Slight systematic underestimation, possibly introduced by the air cavity of the tunnel.



Terrain inversion results

- Proposed a method based on light-guide arrays for low-cost, high-resolution scintillator detectors.
- Built a MuGrid-v2 prototype with a spatial resolution of 4.6 mm
- Performed two outdoor imaging experiments with good agreement to known targets.
- 60cm × 60cm prototype is under development with upgraded materials and better spatial resolution is expected.



Broad horizons, boundless possibilities



Thanks